

1 **Water exchange between the Gulf of California and the Pacific Ocean: results from a**  
2 **one-year global HYCOM simulation**  
3  
4  
5  
6

7 Gonzalo Acosta-Solís<sup>1</sup> (ORCID 0009-0004-7482-6566), Manuel López-Mariscal<sup>1</sup> (ORCID 0000-0002-  
8 0449-8016) y Luis Zamudio<sup>2</sup> (0009-0005-9203-8106)  
9

10  
11  
12 **Abstract**  
13

14 The mean and seasonal water exchange between the gulf of California and the Pacific Ocean  
15 (PO) are analyzed with a one-year global HYCOM simulation. At the mouth of the gulf there  
16 are six alternating layers of inflow and outflow of mean transport with inflow in the uppermost  
17 layer (0-68 m) and the largest outflow in the second layer (68-198 m). The three uppermost  
18 layers have the largest mean transports, and they can be identified more than two thirds  
19 along the length of the gulf with approximately the same thickness. The difference in the  
20 transport between the interior of the gulf and the transport at the mouth in the upper layer,  
21 shows that there must be an upward mean transport (upwelling) into the upper layer along  
22 almost the entire length of the gulf. The two deepest layers have smaller mean transports, but  
23 the deepest layer has an outflow that is about half of the inflow of the surface layer implying a  
24 very large vertical transport into that layer. We obtained the seasonal exchange by fitting  
25 annual and semiannual harmonics to the monthly mean transports in each layer. The maxima  
26 and minima of the seasonal exchange are larger than the mean and they occur in summer  
27 and autumn showing that most of the exchange with the PO occurs during those two  
28 seasons. The maximum inflow ( $\sim 0.8$  Sv,  $1 \text{ Sv} = 1 \times 10^6 \text{ m}^3/\text{s}$ ) in the upper layer occurs at the  
29 beginning of July and the maximum outflow at the beginning of November ( $\sim 0.4$  Sv). The  
30 transport in the second layer is out of the gulf all year round. The fourth layer (380-822 m) has  
31 the smallest mean transport of all layers but, together with the first layer, has the largest  
32 seasonal transport. The net outflowing transport is about 0.2972 Sv, which gives a turnover  
33 time of approximately 14 years for the gulf.  
34

35 Key words: Gulf of California, exchange with the Pacific Ocean, seasonal variations, turnover  
36 time  
37  
38  
39  
40  
41  
42  
43

---

<sup>1</sup> CICESE, Depto. de Oceanografía Física, Ensenada, Baja California, México

<sup>2</sup> Florida State University, Center for Oceanic-Atmospheric Prediction Studies, Tallahassee, Florida, USA

## Resumen

Se analiza el intercambio medio y estacional entre el Golfo de California y el Océano Pacífico (OP) utilizando una simulación anual del modelo global HYCOM. En la boca del golfo se encontraron seis capas que alternan entre transporte medio de entrada y salida, con flujo de entrada en la capa superficial (0-68 m) y de salida en la segunda capa (68-198 m). Las tres capas superiores tienen los transportes más grandes y se pueden identificar más de dos tercios de la longitud del golfo con un espesor aproximadamente constante. La diferencia en el transporte superficial entre el interior del golfo y el de la boca, muestra que existe un transporte vertical medio hacia arriba (surgencia) hacia la capa superficial en casi toda la longitud del golfo. Las dos capas más profundas tienen transportes más pequeños, pero la más profunda tiene un transporte hacia afuera que es aproximadamente la mitad del transporte entrando por la capa superficial, lo cual implica que hay un transporte vertical intenso hacia esa capa. Obtuvimos el intercambio estacional ajustando armónicos anuales y semianuales a los promedios mensuales del transporte en cada capa. Los máximos y mínimos del intercambio estacional son más grandes que la media, y los valores extremos más grandes ocurren en verano y otoño, mostrando que durante esos periodos se da el intercambio más fuerte con el OP. El transporte de entrada máximo ( $\sim 0.8$  Sv,  $1 \text{ Sv} = 1 \times 10^6 \text{ m}^3/\text{s}$ ) en la capa superficial ocurre a principios de julio, y el máximo de salida a principios de noviembre ( $\sim 0.4$  Sv). El transporte en la segunda capa es de salida durante todo el año. El transporte medio en la cuarta capa es el más pequeño, pero junto con la primera capa, tiene los transportes estacionales más grandes. El transporte neto de salida son  $0.2972$  Sv, lo cual da un tiempo de residencia del agua del golfo de aproximadamente 14 años.

Palabras clave: Golfo de California, intercambio con el Océano Pacífico, variaciones estacionales, tiempo de residencia.

## 70 1. Introduction

71 It has long been recognized that the Pacific Ocean (OP) exerts an important dynamical and  
72 thermodynamical influence in the Gulf of California (GC), ranging in time scales from the tides  
73 to the interannual (e.g., Baumgartner and Christensen, 1985; Marinone, 1997; Ripa, 1997;  
74 Lavín and Marinone, 2003). The gulf is an evaporative basin which losses, on average, about  
75 1 m of water per year through the surface (Castro et al., 1994; Berón-Vera and Ripa, 2000),  
76 which implies an average, net incoming transport of about  $5 \times 10^{-3}$  Sv ( $1 \text{ Sv} = 1 \times 10^6 \text{ m}^3/\text{s}$ ).  
77 However, unlike the Mediterranean and Red Seas, the gulf gains heat through the surface  
78 (Bray, 1988), and this has prompted the idea that the gulf may have an estuarine-like  
79 circulation with outflow in a surface layer and inflow in a layer below, with a near-surface  
80 seasonally reversing layer (Bray, 1988; Lavín and Marinone, 2003). But the gulf has no sill at  
81 its mouth, and therefore it has an unrestricted exchange with the PO. This unrestricted  
82 communication with the PO, together with the complex circulation around its mouth (Kessler,  
83 2006; Portela et al., 2016) and the equatorial influence via coastally-trapped waves (Gómez-  
84 Valdivía, et al., 2015) points to a more complex exchange between the gulf and the PO.

85 Flow at the mouth of the gulf has been studied mainly using hydrographic observations and  
86 associated geostrophic velocities (e.g., Mascarenhas et al., 2004; Castro et al., 2006; Castro  
87 et al., 2017; Collins and Castro, 2022). Mascarenhas et al. (2004) were the first to calculate a  
88 mean geostrophic section across the gulf's mouth and they found a broad region of inflow  
89 along the Sinaloa (mainland) coast and outflow along de Baja California (BC) coast, with two  
90 narrower bands of alternating flow between the broader regions of inflow and outflow adjacent  
91 to the coasts. Recently, Collins and Castro (2022) using more observations, calculated the  
92 mean geostrophic currents at the mouth. They found the same general pattern of cyclonic  
93 flow, but without the mid-sections of inflow and outflow bands. Their mean section was,  
94 roughly, evenly divided between inflow to the east and outflow to the west. They also  
95 calculated the laterally integrated transport across the mouth of the gulf and found a mean  
96 inflowing layer in the upper 150 m and an outflowing layer below down to 400 m. Zamudio et  
97 al. (2008) calculated mean, and monthly mean meridional velocities at the mouth of the gulf  
98 using HYbrid Coordinate Ocean Model (HYCOM) simulations but no integrated transports  
99 across the mouth were reported. The mean meridional velocities did capture the general  
100 cyclonic pattern with inflow through the east and outflow to the west.

101 Despite these very important observational and modelling efforts there has been no articles  
102 reporting the vertical structure of the mean volume exchange with the PO throughout the  
103 water column at the mouth of the gulf. Moreover, we do not know what the seasonal variation  
104 of this exchange, nor the along-gulf structure of the volume transport is. In this article we give  
105 a description of the mean and seasonal exchange of the gulf with the PO; and also look into  
106 the along-gulf structure of the volume transport using a one-year, global simulation of the  
107 HYCOM. One important advantage of using a global simulation is that it includes the  
108 phenomena of the eastern tropical Pacific which influence the exchange with the gulf. In the  
109 next section we give a brief description of the model; in section three we describe the results;  
110 and in section four we discuss the results and give concluding remarks.

111

## 112 2. The HYCOM simulation, and methods

113 The HYCOM is a hydrostatic ocean model which, as its name indicates, employs a hybrid  
114 vertical coordinate system. The model uses isopycnic (density tracking) coordinates in most  
115 of the open stratified ocean, but switches to z-coordinates (fixed water depths) in the upper  
116 mixed layer. It also uses sigma (terrain following) coordinates in shallow regions. The model  
117 has been extensively used by the ocean modelling community and a fuller description can be  
118 found in Zamudio et al. (2008) and references therein. In this article we use a one-year  
119 simulation known as expt\_06.1, which is forced at the surface with hourly heat fluxes and  
120 wind stress from the atmospheric Navy Global Environmental Model (NAVGEM). The model  
121 also includes tidal forcing by the five largest constituents ( $M_2$ ,  $S_2$ ,  $N_2$ ,  $K_1$ , and  $O_1$ ). Tidal forcing  
122 is particularly important in the gulf, which has large tidal currents in the northern gulf around  
123 the sills of the large mid-riff islands (López et al., 2021; and see figure 1 for the location of the  
124 islands). The model has 41 vertical layers (35 at the mouth of the gulf), and a horizontal  
125 resolution of  $1/12.5^\circ$  which is a about an 8 km meridional increment at the mouth of the gulf.  
126 Details on the initial conditions and spin-up of the simulation; and when the tides are turned  
127 on, are given in Bujisman et al. (2017). The simulation comprises one year from October 1<sup>st</sup>,  
128 2011 to September 30, 2012, and fields are available hourly. The simulation does not include  
129 data assimilation. All results presented in this article are from this HYCOM simulation.

130 Using the hourly fields, we calculated instantaneous zonal transport by multiplying the  
131 meridional velocity by the model's variable layer thicknesses. The model velocities are always  
132 located at the center of any existing layer, whether the layer is isopycnic (variable depth and  
133 location) or fixed water depth. We then obtained a temporal mean of the transport which was  
134 then integrated across the mouth of the gulf, and across zonal sections inside the gulf, to  
135 obtain vertical profiles of the transport. We also obtained zonal sections of vertically  
136 integrated transport across the mouth of the gulf over the whole depth range or over certain  
137 depth ranges where there is mean inflowing or outflowing transport.

138 The seasonal fields were obtained by first calculating monthly averages from the hourly fields.  
139 Months were calculated starting from October 1<sup>st</sup>, 2011, but they were of equal duration (30.5  
140 days) so that no month had more observations than other. The seasonal fit was made to a  
141 constant mean, and to annual and semiannual harmonics according to

$$142 \quad Q = A_0 + A_1 \cos(\omega t - \theta_1) + A_2 \cos(2\omega t - \theta_2) .$$

143 The coefficients ( $A_0, A_1, A_2$ ) and the phases ( $\theta_1, \theta_2$ ) were obtained by a least square fit to the  
144 monthly data at times  $t$ ; and  $\omega$  represents the annual frequency.  $Q$  represents velocity or  
145 transport.

146 The transport at the mouth and at the interior of the gulf was obtained along zonal sections  
147 spanning the width of the gulf. The zonal section at the mouth of the gulf is shown in figure 1.  
148 Therefore, we calculated the inflowing or outflowing meridional transports across zonal  
149 sections. However, given the time scales involved in this study (mean and seasonal), the  
150 conservation of mass implies that this meridional transport integrated across the gulf (black  
151 lines is figure 1) is equal to the transport at the corresponding across-gulf (perpendicular to  
152 the axis of the gulf) section starting at the same grid point on the peninsular side of the mouth  
153 of the gulf (e.g., red line in figure 1). Similar zonal sections were used by Zamudio et al.  
154 (2008, 2010, 2011) to show flow into and out of the gulf.

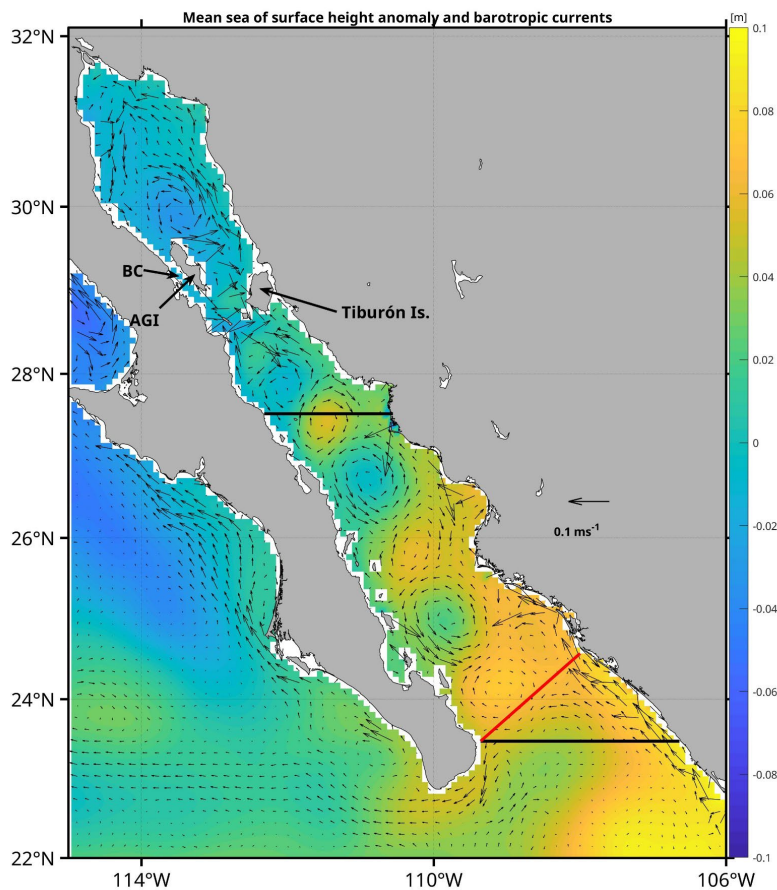


Figure 1. Modeled yearly mean sea surface height and barotropic currents in the gulf of California. The zonal sections (black lines) across the gulf, is where vertical profiles of transport appearing in figure 3 were calculated. The across-gulf section corresponding to the mouth of the gulf (red line) is also shown. AGI and BC stand for Ángel de la Guarda Is., and Ballenas channel, respectively.

155

156 3. Results

157 3.1 Mean fields

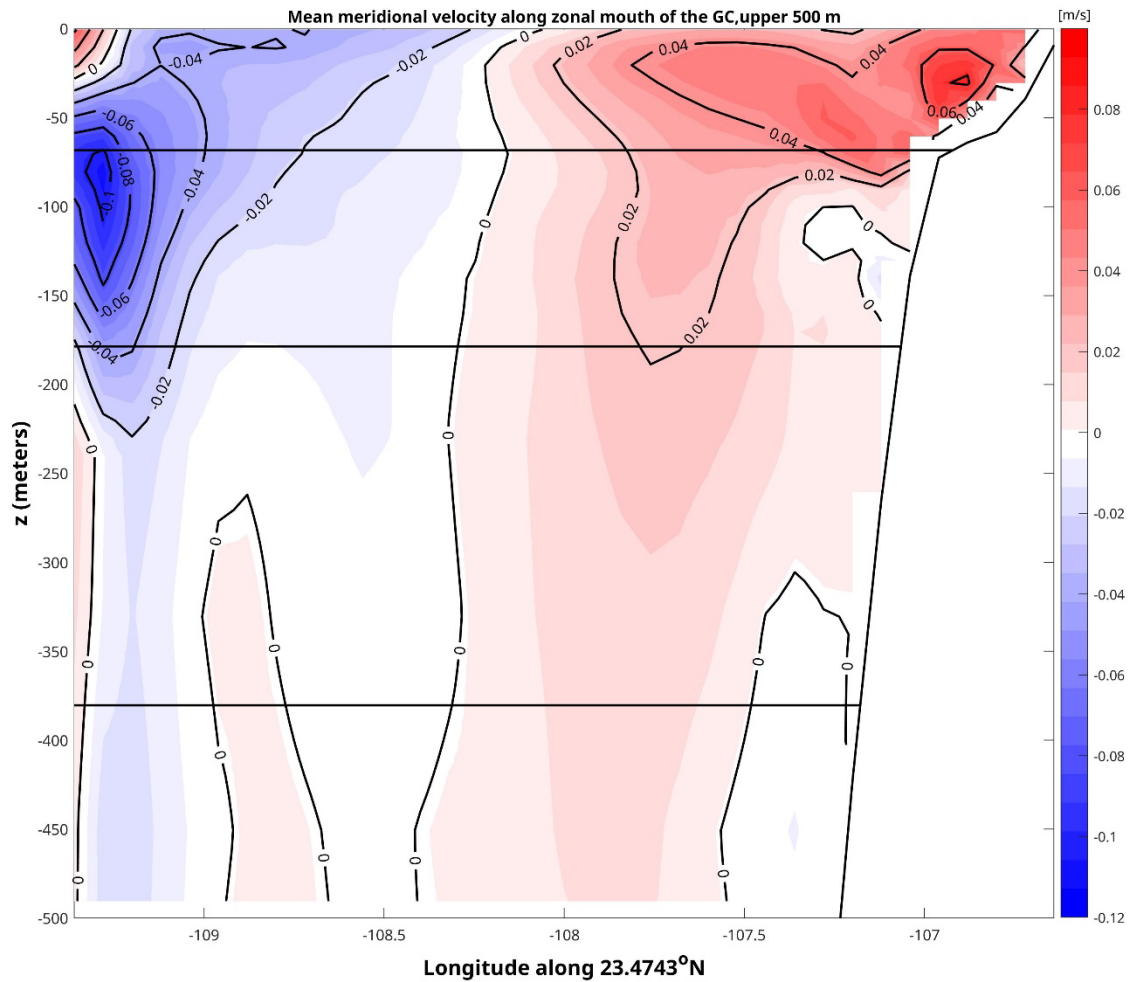
158 Figure 1 shows the yearly mean of sea surface height and barotropic currents in the gulf. The  
 159 most conspicuous feature is the train of eddies with alternating sense of rotation, spanning  
 160 the whole length of the gulf, starting with a relatively weak anticyclonic eddy just north of the  
 161 zonal section at the mouth. The eddies in several parts of the gulf have been documented in

162 observational and modelling studies (e.g., Lavín et al., 1997; Pegau et al., 2002; Martínez  
163 Alcalá, 2002; Zamudio et al., 2008; Lavín et al., 2013), but this is the first time that they have  
164 been shown to span the whole length of the gulf in a one-year mean numerical simulation.  
165 The northernmost cyclonic eddy, to the north of Ángel de la Guarda Island (see figure 1) has  
166 been shown to reverse signs seasonally, being cyclonic in summer and anticyclonic in winter  
167 (Lavín et al., 1997). The eddy in the northern gulf does reverse sign in this simulation (not  
168 shown but see Acosta-Solís, 2023) being anticyclonic in fall; cyclonic in spring and summer,  
169 and not well defined in winter. The mean, however, turns out to show a cyclonic eddy for this  
170 particular yearly simulation. Figure 1 also shows a strong Mexican coastal current (MCC)  
171 entering the gulf along the eastern coast. However, in the mean field, the MCC does not show  
172 up as a recognizable feature inside the gulf as the train of eddies dominate the mean  
173 circulation and give rise to alternating flows along the eastern coast.

174 The mean meridional velocity at the mouth of the gulf in the upper 500 m is shown in figure 2.  
175 The mean velocity field is approximately evenly divided in inflow through the eastern half and  
176 outflow in the western half. The core of the outflow is deeper ( $\sim 80$  m), more intense, and  
177 localized on the western side, than the inflow on the eastern side ( $\sim 25$  m). There are,  
178 however, some smaller scale, localized flow reversals. Most notably a relatively small and  
179 intense inflow on the surface western side corner, and two weaker outflows on the eastern  
180 coast centered around 125 and 450 m. It is rather remarkable that the general, large-scale  
181 pattern of inflow and outflow in figure 2 resembles very well the mean geostrophic velocity  
182 calculated by Collins and Castro (2022) based on 18 cruises taken on different years (see  
183 their figure 3d). The agreement between the modeled and the observed fields includes the  
184 depth of the outflow core on the western side. The almost evenly divided outflow and inflow in  
185 the western and eastern sides, respectively, is also obtained by Collins et al. (1997) for four  
186 individual sections.

187 The laterally integrated transport at zonal sections results in a vertical profile of transport. Two  
188 profiles, one at the mouth and another one around a mid-gulf section (see figure 1) are shown  
189 in figure 3. At the mouth the transport is arranged in six layers of alternating inflow (at the  
190 top) and outflow layers. The same six layers are found in the mid-gulf section, but the lowest  
191 three layers have a very small transport. It is important to mention that since the values in  
192 figure 3 are already in Sverdrups, the total transport in each of the six layers is the sum of the

193 transports in each of the model's layers (given by the circles in figure 3) which are inflowing or  
194 outflowing; and, therefore, the transport is not proportional to the area between the curve and  
195 the vertical axis. The values of the transport in each of the inflowing and outflowing layers,  
196 together with their standard errors and depth ranges, are given in table 1. At the surface there  
197 is mean inflow of Pacific waters, followed below by an outflow which should include GC



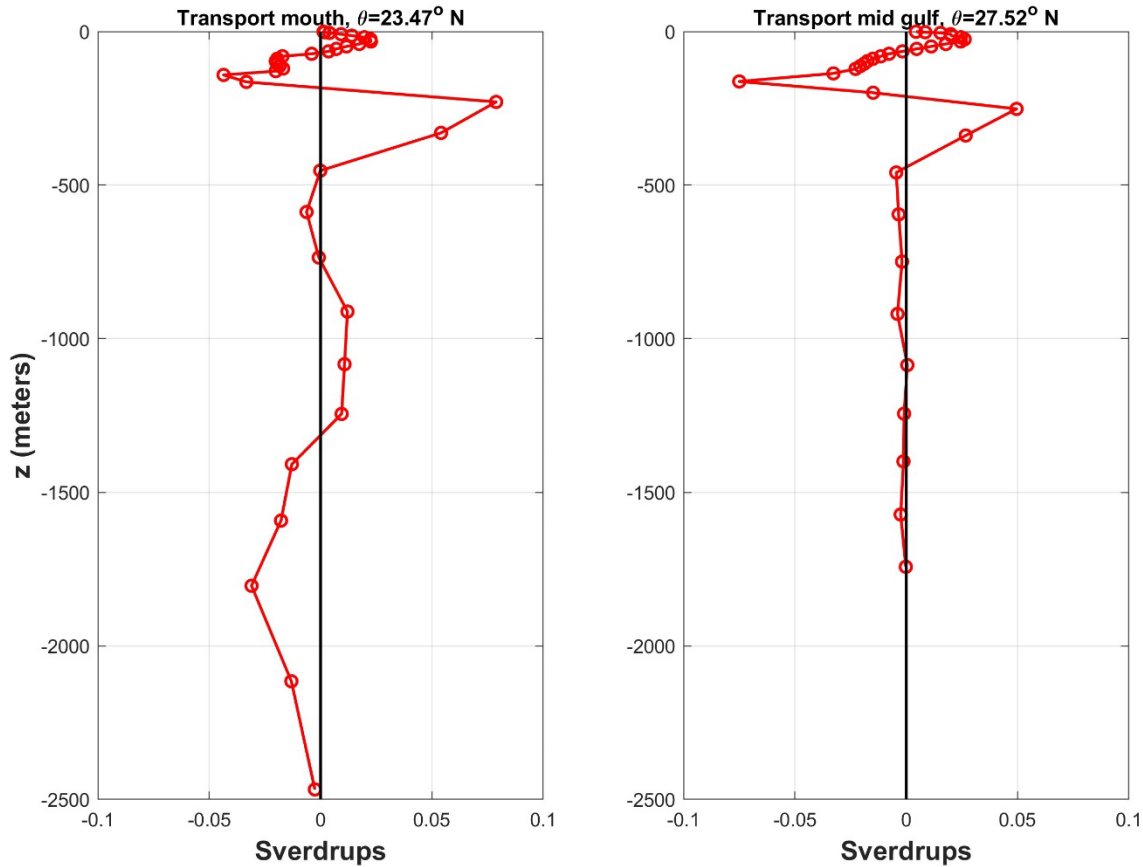
198

Figure 2. Modeled zonal section of the annual mean meridional velocity at the mouth of the gulf (upper 500 m). The horizontal lines are the boundaries of the first three layers in which the transport is inflowing or outflowing (see figure 3 and table 1). Inflow is shaded red, and outflow white and blue. Contour interval is 0.02 m/s.

199

200 waters, possibly mixed with Pacific waters from below and/or above. The third inflowing layer  
201 is consistent with inflow of subsurface subtropical water from the Pacific Ocean (Castro et al.,

202 2006; Portella et al., 2016). The fourth layer has a very small mean transport, and the  
 203 inflowing fifth layer would be consistent with the inflow of Pacific intermediate water (Portela  
 204 et al., 2016). The deepest layer has a net outflowing transport, necessarily composed of  
 205 Pacific deep water. Note that the transport in the deepest layer is more than half of the  
 206 transport of the surface layer, and it implies a mean downwelling from the layer above. Mean  
 207 meridional velocities averaged across the zonal section are small ( $\approx 0.01$  m/s, not shown) but  
 208 transports are significant; for example, mean, across-gulf averaged velocities in the lowest  
 209 two layers are less than 1 mm/s, but their transports are significant. The first four layers in the  
 210 mid-gulf section have approximately the same depth ranges, and the first two have similar  
 211 transports, as the corresponding ones at the mouth. The transport in the outflowing fourth  
 212 layer of the mid-gulf section is significantly greater than the corresponding one at the mouth.



213

Figure 3. Modeled across-gulf integrated transport at zonal sections at the mouth of the gulf (left) and at a mid-gulf section (right). Symbols represent the transport at the model's vertical layers. Locations of the zonal sections are shown in figure 1.

214 The annual mean, vertically integrated meridional transport at the zonal section across the  
 215 mouth of the gulf is shown in figure 4, together with the transports at each of the six inflowing  
 216 and outflowing layers appearing in figure 3 and table 1. The bulk of the vertically integrated  
 217 transport enters the gulf through half of the section on the eastern side, whereas most of the  
 218 outflow takes place in a more concentrated core of larger transports next to the western side.  
 219 These two inflowing and outflowing regions adjacent to the coasts are separated by two less  
 220 intense bands of outflowing and inflowing transport (see figure 4). The same general pattern

221 Table 1. Modeled transports in the inflowing and outflowing layers shown in figure 3. Positive  
 222 values are transport into the gulf.

Layer	Mouth		Mid-gulf	
	Depth range (m)	Transport (Sv)	Depth range (m)	Transport (Sv)
1	0-68	$0.135 \pm 0.114$	0-59	$0.177 \pm 0.073$
2	68-179	$-0.213 \pm 0.060$	59-211	$-0.236 \pm 0.059$
3	179-380	$0.133 \pm 0.070$	211-381	$0.077 \pm 0.018$
4	380-822	$-7.2 \times 10^{-3} \pm 0.11$	381-994	$-0.012 \pm 0.022$
5	822-1325	$0.032 \pm 0.07$	994-1147	$7.04 \times 10^{-4} \pm 0.007$
6	1325-2621	$-0.077 \pm 0.091$	1147-1725	$-5.32 \times 10^{-3} \pm 0.007$

228

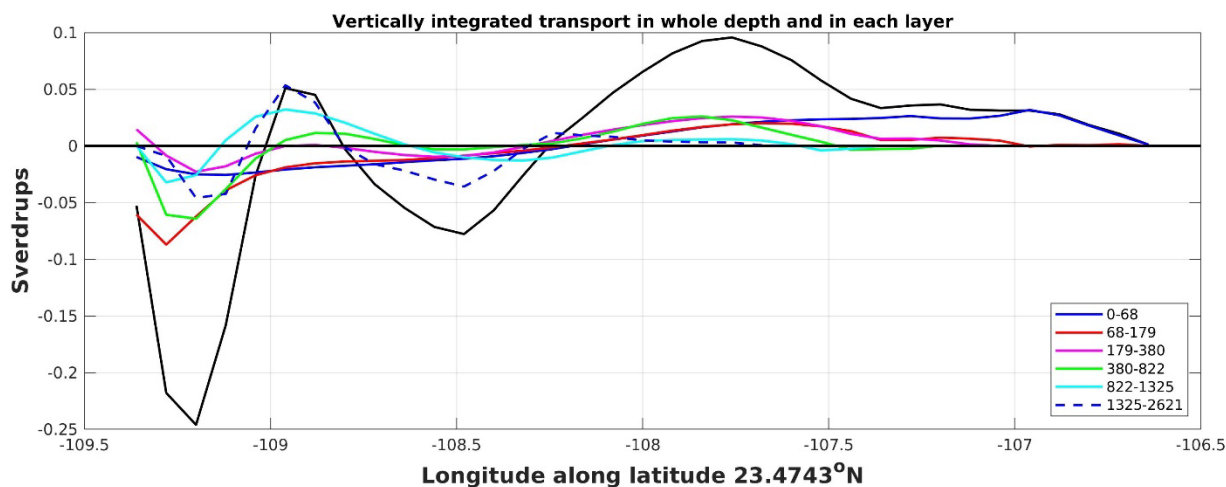
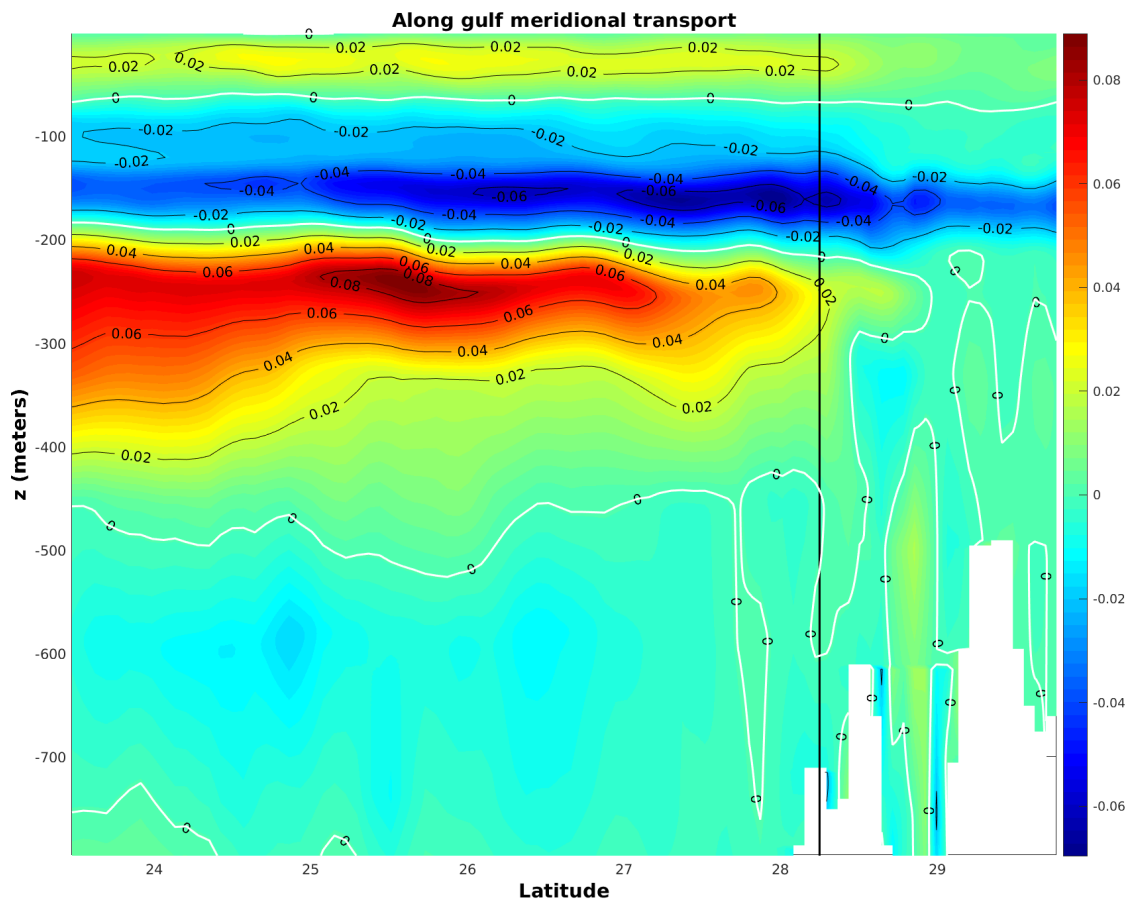


Figure 4. Modeled annual mean, vertically integrated transport across the zonal section at the mouth of the gulf (thick black line). The colored and/or dashed lines are the transports at the six different layers where there is inflow or outflow mean transport (see figure 3 and table 1). The color code of the six layers and their depth range is given in the inset.

229 of broad inflow on the eastern side and concentrated outflow in the western side is present in  
 230 all six layers where the laterally integrated transport is inflowing or outflowing. Most of the  
 231 inflow on the eastern side occurs in the first layer, whereas the largest concentrated outflow  
 232 on the western side occurs in the second and fourth layers.

233 The across-gulf, integrated meridional transport *along the gulf*, down to 800 m, is shown in  
 234 figure 5, which is constructed from transport profiles as the ones appearing in figure 3, but at  
 235 all latitudes of the model. The along-gulf section is plotted to 29.76°N. Northward of this  
 236 latitude the gulf shallows significantly and the two deeper layers (roughly below 200 m)



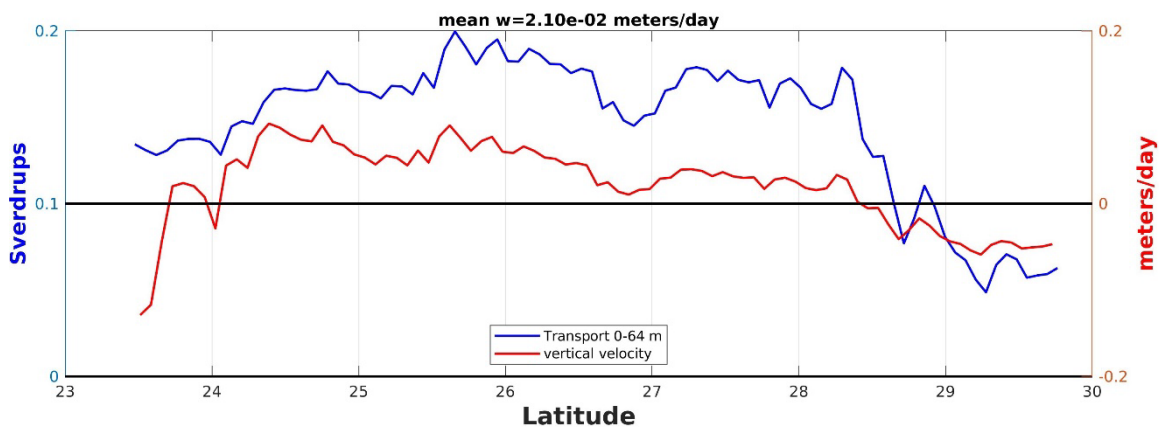
237  
 238 Figure 5. Modeled along-gulf, mean meridional transport integrated in zonal sections along  
 239 the gulf. Contours of zero transport are white. The black vertical line marks the southernmost  
 240 sill that separates the southern gulf from Ballenas channel. Contour interval is 0.02 Sv. The  
 241 field has been smoothed with a three-point running mean.

242

243 start losing their continuity, therefore it is difficult to identify inflowing and outflowing layers in  
 244 the vertical. The most remarkable feature of this figure is that the first four inflowing and  
 245 outflowing layers preserve their continuity and approximate depth range, almost all of the  
 246 gulf's length. In particular, the inflowing surface layer, of approximately 60 m depth, remains  
 247 almost constant throughout the length of the gulf.

248 The meridional transport in the first layer shown in figure 5 is shown in figure 6. Note that the  
 249 transport is everywhere positive (into the gulf) in the first layer. The difference in transport of  
 250 the first layer, between the interior points and the transport at the mouth gives the average  
 251 vertical transport into the first layer. Dividing the vertical transport by the gulf's area up to the  
 252 interior point gives the average vertical velocity between the mouth and the interior point. This  
 253 mean vertical velocity is also shown in figure 6 and is almost everywhere positive indicating  
 254 mean upwelling into the surface layer. The mean vertical velocities are small, but upwelling

255



256

257 Figure 6 Modeled mean meridional transport in the zonal sections which span from the BC  
 258 coast to the continental coast in the first layer (blue curve, left axis); and modeled mean  
 259 vertical velocity between the given latitude and the mouth of the gulf (red curve, right axis).

260

261 may be concentrated in certain areas of the gulf such as the western and eastern coasts; and  
 262 in Ballenas Channel (Badan-Dangon, et al., 1985; López et al., 2006).

263

264

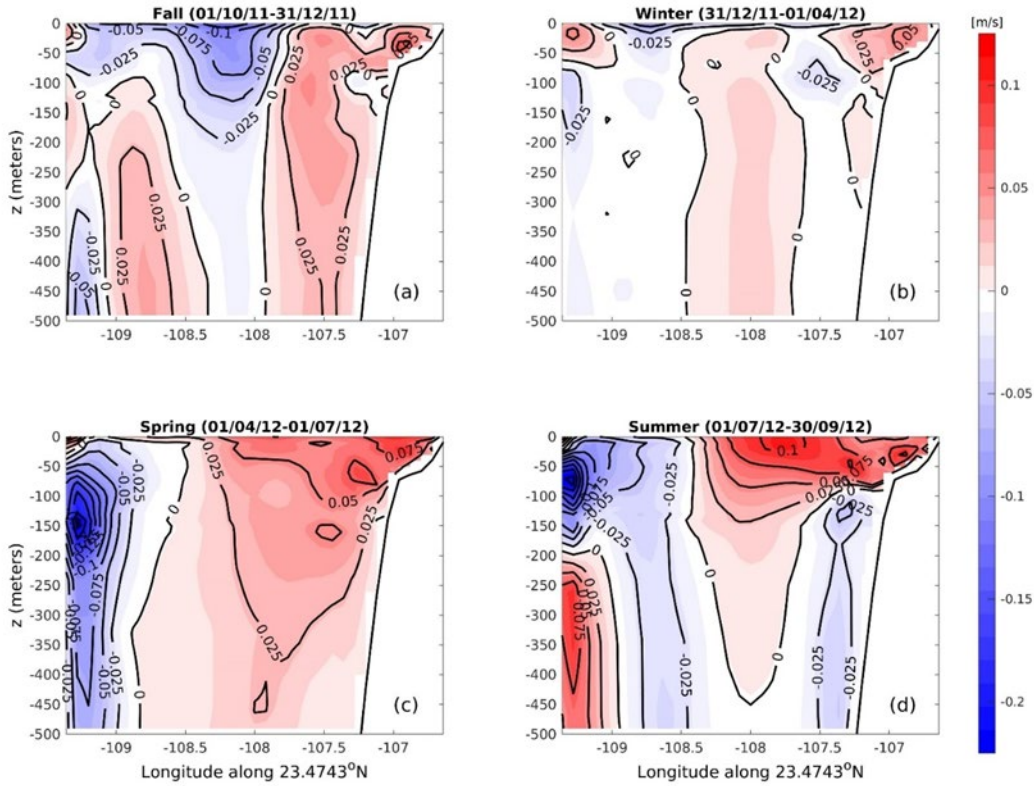
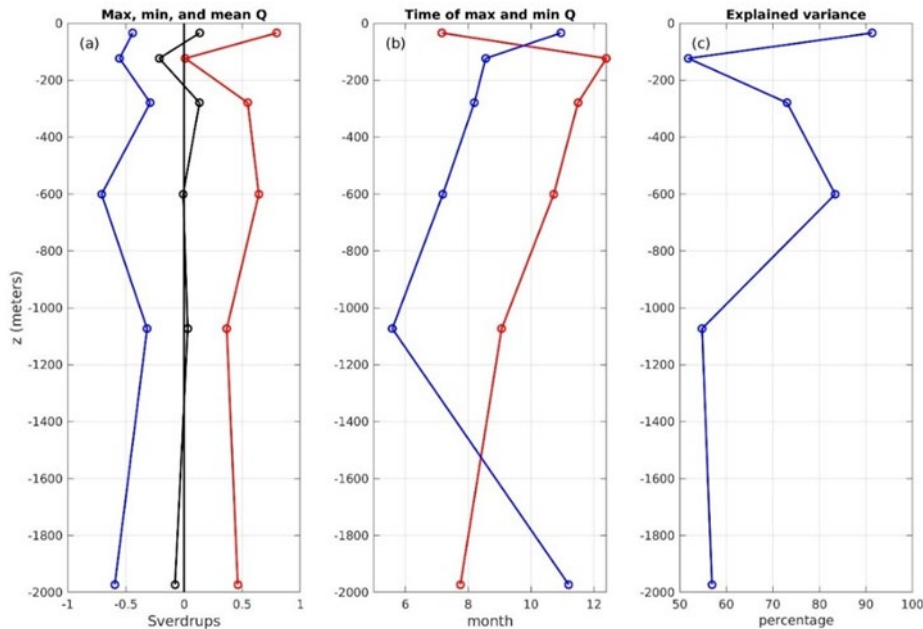


Figure 7. Modeled seasonal zonal sections of meridional velocity along the mouth of the gulf. (a) fall; (b) winter; (c) spring; and (d) summer. Inflow is shaded red, and outflow white and blue. Contour interval is 0.025 m/s.

265 3.2 Seasonal cycles

266 Seasonal zonal velocity sections at the mouth of the gulf are shown in figure 7. Fall starts on  
 267 Oct. 1st, 2011 and all seasons have the same duration (91.5 days). In general, there is  
 268 surface inflow through the eastern side and surface outflow through the western side,  
 269 consistent with the cyclonic circulation of the barotropic currents (figure 1). However, there  
 270 are noticeable smaller scale seasonal patterns. All year there is a localized small inflow on the  
 271 surface western corner, which is largest in winter, in turn, it is this season which has the  
 272 smallest exchange velocities between the gulf and the Pacific Ocean. The largest inflow is  
 273 always localized in the eastern shelf. Spring and summer appear as the seasons with the  
 274 largest exchange velocities, and with a strong localized subsurface core of outflowing waters  
 275 in the western side. Maximum, mean outflow is shifted towards the surface and away from  
 276 the western coast in fall and winter.

277 Figure 8a shows the maximum and minimum values (including the mean) of the laterally  
 278 integrated seasonal transport at the mouth, in each of the six layers appearing in figure 3 and  
 279 table 1. The mean is also plotted to compare with the amplitudes of the seasonal cycle. In all  
 280 cases the range of the seasonal cycle is larger than the mean, and, in general, they are fairly  
 281 uniform (around 0.5 Sv) in the vertical, with the exception of the maximum value in layer 2



282

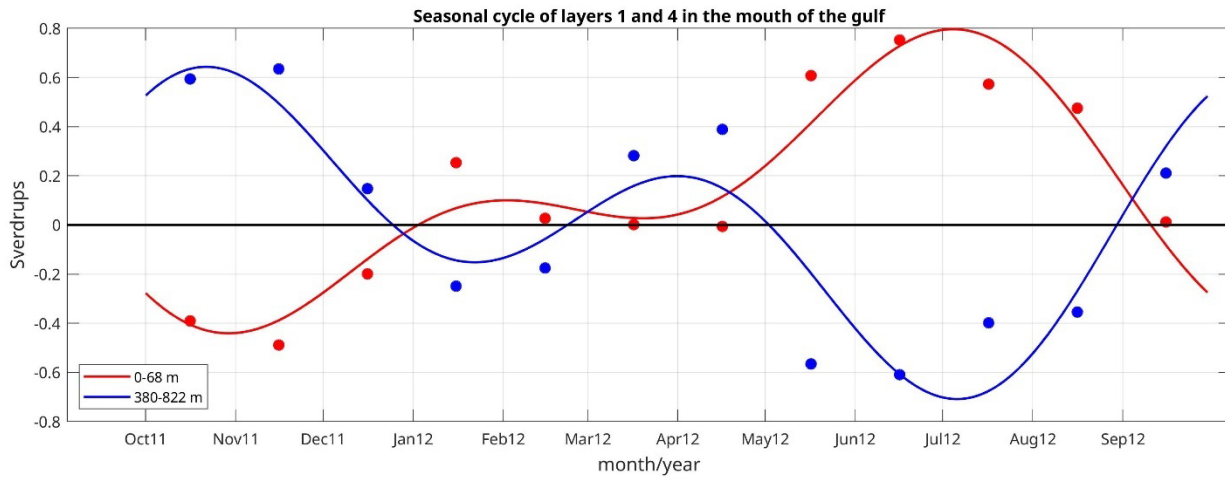
283 Figure 8. (a) Vertical profiles of the minima and maxima of the seasonal cycle (including the  
 284 mean) and the mean (black line) of the layers appearing in table 1 and figure 3 at the mouth.  
 285 (b) Time of occurrence along the year of the minima (blue line) and maxima (red line) of the  
 286 seasonal cycle corresponding to (a). January 1st corresponds to 1.0. (c) Variance explained  
 287 by the seasonal fits. All results are from the model.

288

289 which is shifted to the left by the large negative mean value. The seasonal cycle in the second  
 290 layer is essentially outflowing all year round. The largest ranges in the seasonal cycle are in  
 291 layers 1 and 4. Figure 8b shows the time of the maxima, and minima of the seasonal cycle,  
 292 which are separated by periods ranging from about 2.5 months (deepest layer) to 4.7 months  
 293 (layer 1). The time period between minima and maxima remains almost constant at about 3.5  
 294 months between layers five to two. The time of occurrence of the minima and maxima is

295

296 shifted forward in time as the year progresses from layers five to two. In the surface layer the  
 297 minimum and maximum are significantly shifted in time, becoming out of phase with the  
 298 layers two to five. In particular, layers one and four are 180° out of phase as can be seen in  
 299 the corresponding seasonal cycles in figure 9. Maximum inflow (outflow) in layer one (four)  
 300 occurs at the beginning of summer, whereas the corresponding maximum outflow (inflow)  
 301 occurs at the end of October in layer one (four). The variance explained by the seasonal fits in  
 302 each layer is shown in figure 8c. In all layers the variance explained is greater than 50%, and



303

304

Figure 9. Modeled Seasonal cycles of the transports in the surface layer (layer one, red line) and in layer four (blue line) at the mouth of the gulf. The monthly means are shown as dots with the same color as the corresponding seasonal cycles. The depth ranges of the layers are shown in the inset. Tick marks at the beginning of the month.

305

306 it is more than 80% in layers one and four. The annual and semiannual amplitudes and  
 307 phases, together with their errors for all six layers are given in table 2.

308

309

310

311

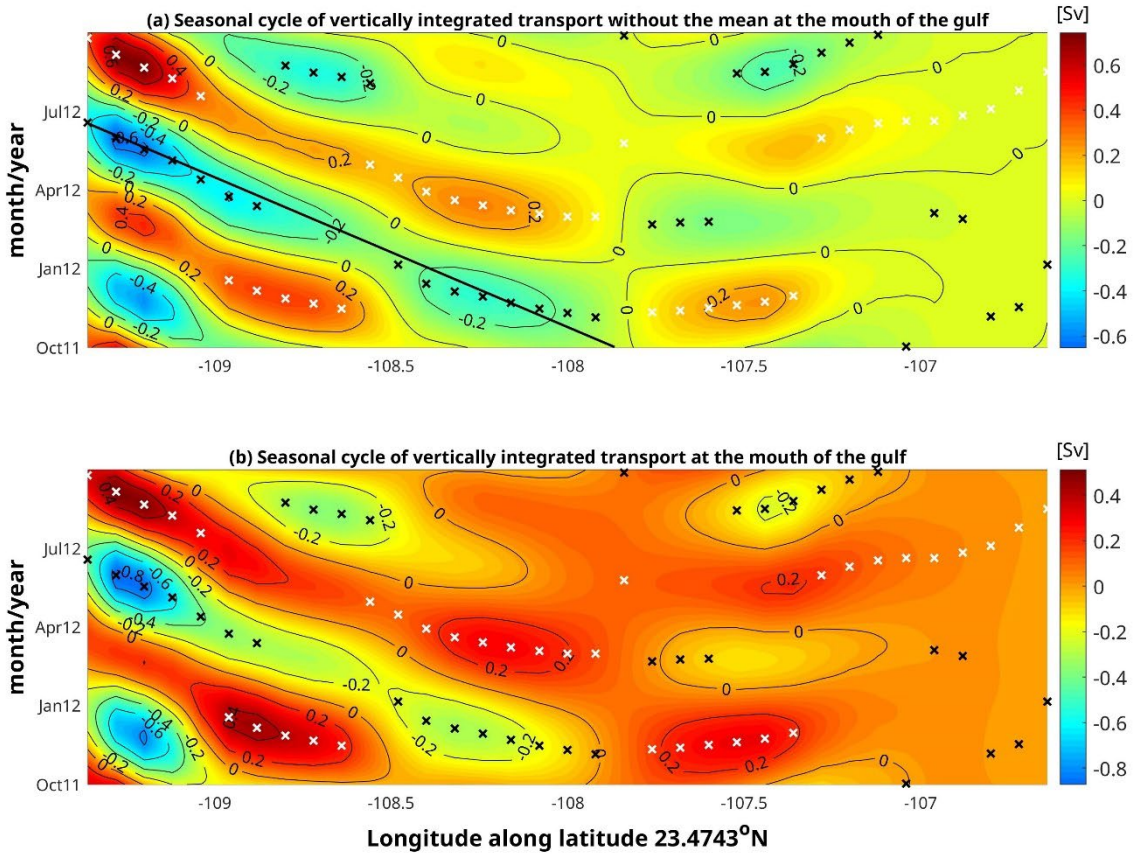
Table 2. Annual and semiannual amplitudes, phases and their corresponding errors for the transport in layers 1 to 6. Errors for amplitude are given in percentage of the amplitude and for phases in days.

Layer	Annual amplitude (Sv)	Error (%)	Annual phase (day/month)	Error (days)	Semiannual amplitude (Sv)	Error (%)	Semiannual phase (day/month)	Error (days)
1	0.44	14	9/6	8	0.28	21	15/7	12
2	0.21	43	5/2	25	0.13	69	21/11	40
3	0.14	56	28/12	32	0.32	25	10/11	15
4	0.36	25	3/12	15	0.41	23	12/10	13
5	0.18	53	13/10	31	0.21	46	25/8	26
6	0.26	53	17/6	31	0.33	42	30/7	24

312

313

314 Figure 10 shows the seasonal cycle of the vertically integrated transport across the mouth of  
 315 the gulf. Figure 10a is without the mean and it clearly shows a semiannual component that is  
 316 dominant along most of the mouth, but most notably west of 108°W. Maximum amplitudes are  
 317 found on the western side adjacent to the coast. Figure 10b shows the same seasonal cycle  
 318 as in 10a but including the mean. The pattern is very similar, but the semiannual cycle is not  
 319 as evident on the eastern side. Actually, including the mean shows that the flow east of  
 320 107°W, over the continental shelf, is into the gulf all year round, and the maximum outflow  
 321 cores on the western side are more pronounced. At the western side there is outflow from  
 322 mid-autumn to mid-winter, and from mid-spring to mid-summer, and inflow during mid-winter  
 323 to mid-spring, and from mid-summer to mid-autumn. The outflow and inflow maxima on the  
 324 western side, occur earlier in the year as one moves east, and there appears to be a  
 325 westward propagation pattern west of 108°W which we have emphasized by drawing a  
 326 sloping line in figure 10a.



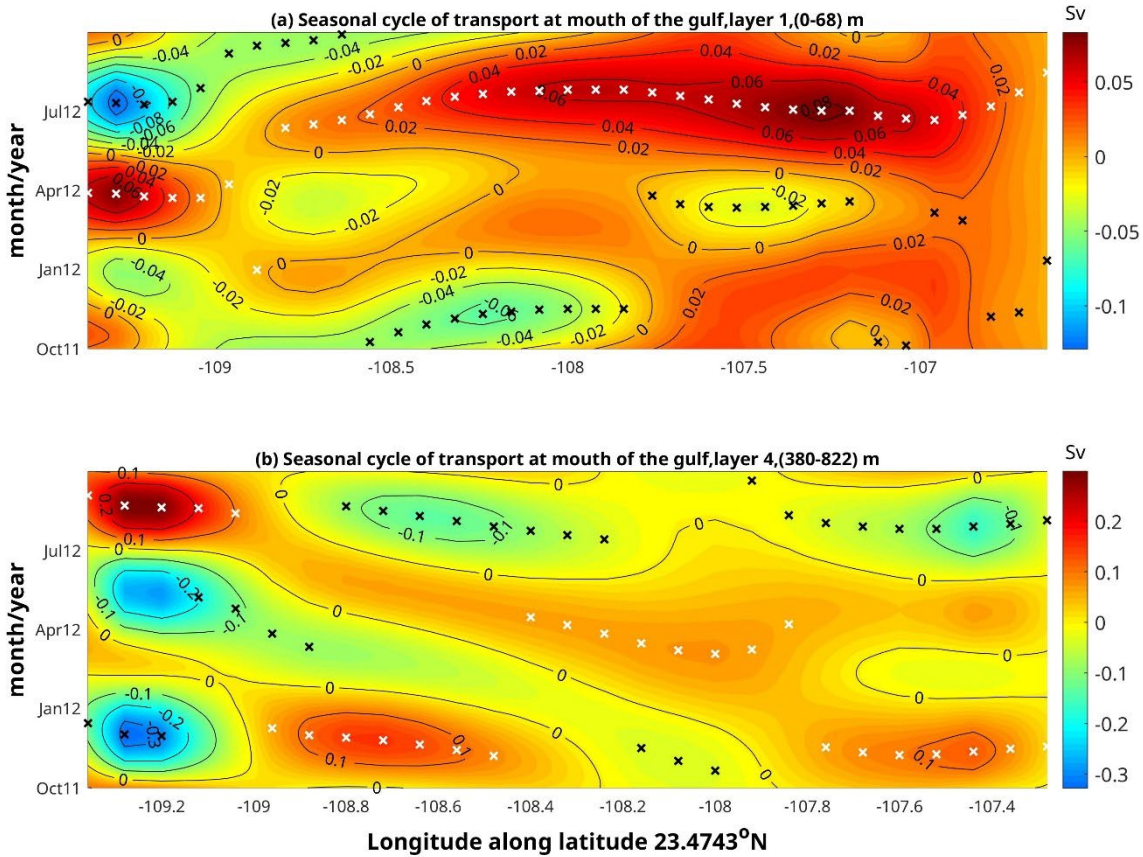
327

328 Figure 10. (a) Modeled seasonal cycle, without the mean, of the vertically integrated transport  
 329 along the zonal mouth of the gulf. (b) As in (a) but including the mean. White (black) crosses  
 330 mark the maximum (minimum) at each location along the mouth. Contour interval is 0.02 Sv.

331

332 Figure 11 shows plots similar to figure 10, but for layers 1 and 4 (see table 1), both including  
 333 the mean. In both layers, there is a strong semiannual component on the western side close  
 334 to the coast (west of 109°W) where localized cores of inflow and outflow alternate throughout  
 335 the year. Plots, similar to the ones in figure 11 but for the other 4 layers (not shown), show  
 336 that the semiannual component on the western side is present at all depths. In layer 1, there  
 337 is inflow almost in the entire section (east of 109°W) during late spring and summer; and all  
 338 year east of 107°W, consistent with figures 7 and 10. The rest of the year, at the mouth, there  
 339 are regions of inflow and outflow in most of the section. In layer four (figure 11b), the  
 340 semiannual component is present in most of the section, which is consistent with the  
 341 amplitudes of the annual and semiannual component for this layer (see table 2). Note that in

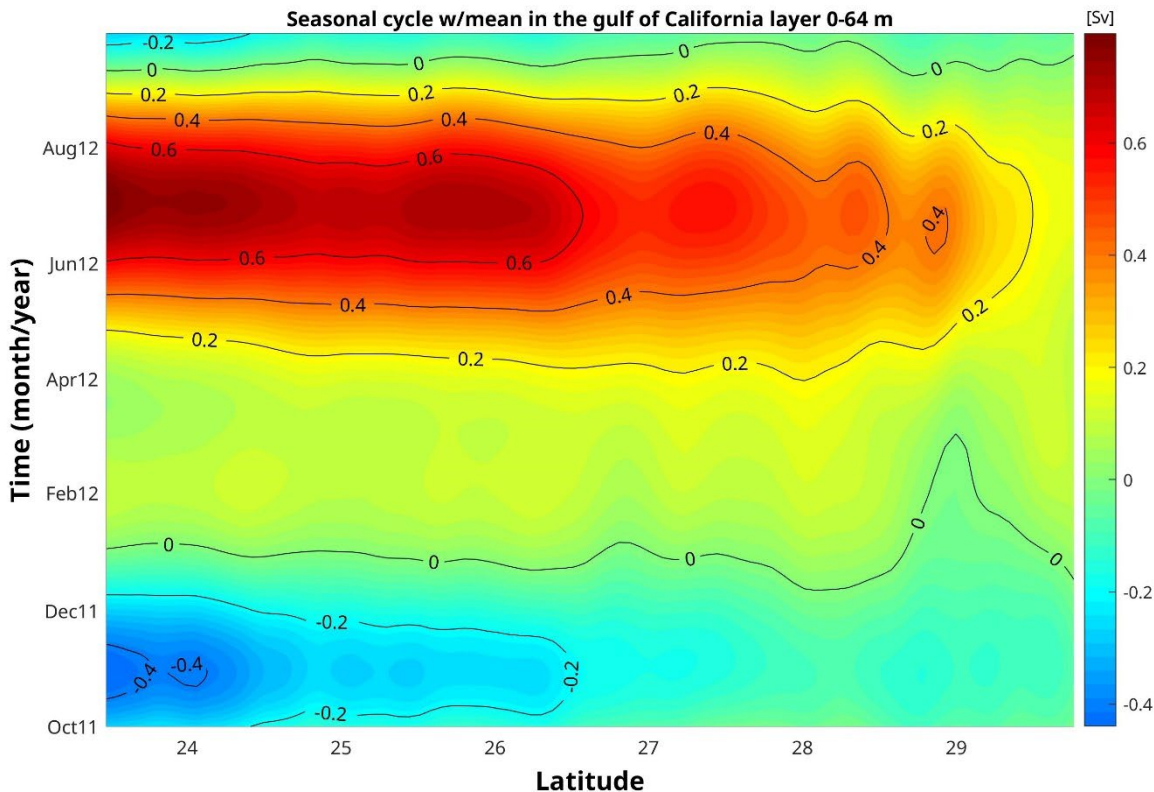
342 layer 4 there is clear evidence of western propagation at the semiannual frequency west of  
 343 about 108°W, however there is no similar evidence in layer 1. Actually, there is only evidence  
 344 of western propagation in layers three to six which does show up when vertically integrating  
 345 all six layers from surface to bottom (figure 10). Note also, that on the western side, where  
 346 there is a clear semiannual component, layers one and four are not quite 180° out of phase,



347  
 348 Figure 11. (a) Modeled seasonal cycle (including the mean) of the vertically integrated  
 349 transport along the zonal mouth of the gulf in layer 1(0-68 m). (b) As in (a) but for layer 4  
 350 (380-822 m). White and black crosses are as in figure 10. Contour interval is 0.02 (0.01) Sv in  
 351 (a) ((b)).

352  
 353 they are more like 90° out of phase. However, when integrated across the mouth of the gulf  
 354 they do become 180° out of phase and are dominated mainly by the annual frequency (see  
 355 figure 9).

356 The seasonal cycle of the mean across-gulf averaged transport *along the gulf* in the first layer  
 357 is shown in figure 12. As is evident in the mouth (figure 9), the transport in the interior of the  
 358 gulf in the first layer, has a predominant annual frequency and is practically in phase all along  
 359 the gulf. Including the mean, there is outflow only during the fall (September to December)  
 360 and inflow the rest of the year. The largest outflow occurs during the end of October and the  
 361 largest inflow at the beginning of summer. The largest inflow and outflow occurs at the



362  
 363 Figure 12. Modeled seasonal cycle (including the mean) of the laterally integrated transport  
 364 along the gulf in the first layer. The field has been smoothed with a three-point running mean.  
 365 The contour interval is 0.2 Sv.

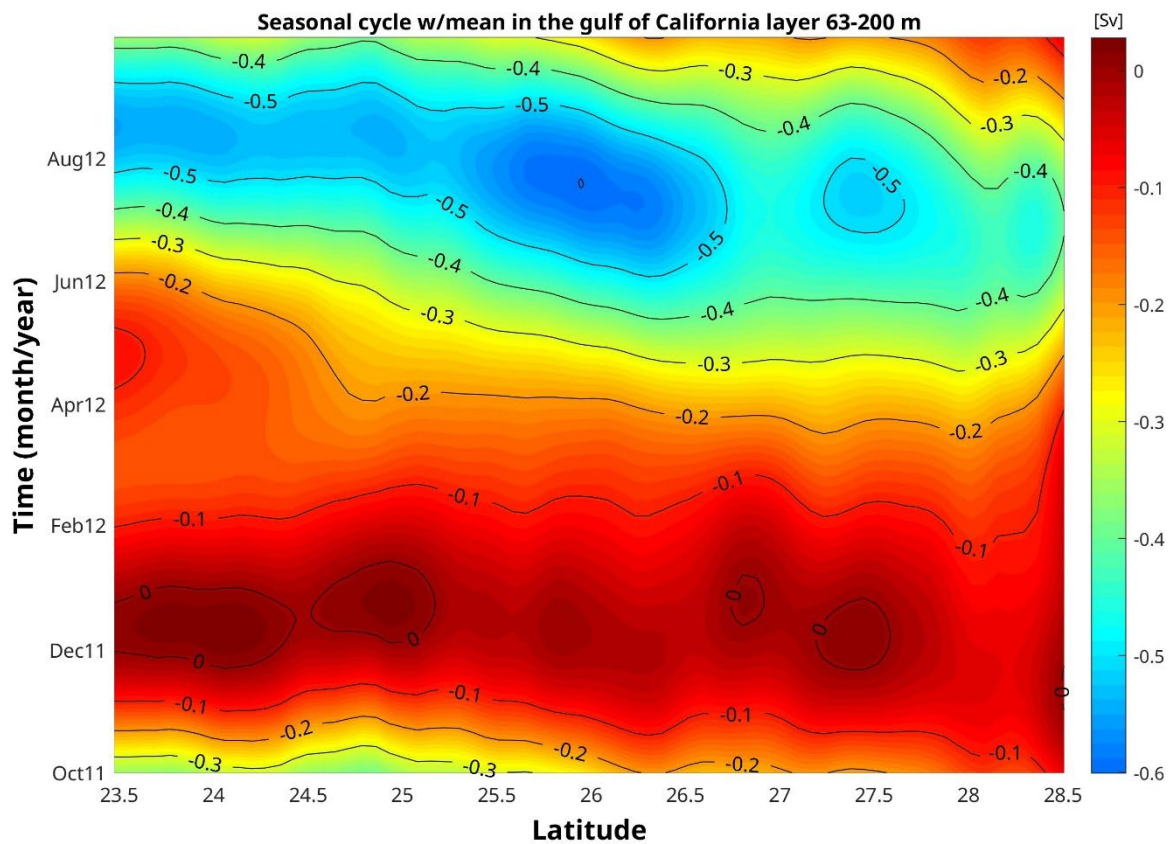
366  
 367 mouth, with a secondary smaller maximum inflow around 26°N. Northward of this latitude,  
 368 inflow and outflow decrease towards the head of the gulf. In the second layer, the seasonal  
 369 cycle including the mean (figure 13), shows that, practically all along the gulf, there is outflow,  
 370 with small pockets of very weak inflow during the end of the fall. There appears to be a small  
 371 phase shift in the maximum outflow during mid-summer, with maximum outflow occurring

372 earlier in the interior of the gulf. Note that the along-gulf extent of the second layer is smaller  
373 than for the first layer because the second layer loses its continuity around 28.5°N (see  
374 figure 5).

375

#### 376 4. Discussion and Concluding Remarks

377 Unfortunately, there are not many observations which we can compare with, especially since  
378 transport averaged across the gulf is difficult to estimate from observations. However, there is  
379 very good agreement with the three layer, near-surface (0-500 m) circulation found by Bray



380

381 Figure 13. As in figure 12 but for the second layer. Contour interval is 0.1 Sv.

382

383 (1988) in the mid-gulf section using geostrophic velocities based on data from several years.  
384 As we did with the model, Bray also found an outflowing subsurface layer (50-250 m) and an  
385 inflowing layer from 250 m down to 500 m. For the surface layer, Bray (1988) did not establish

386 a mean transport but only stated that it reverses with the seasonal winds, flowing towards the  
387 head in summer and towards the mouth in winter. Here we have shown that, in the model, the  
388 net transport in the surface layer is northward and, therefore, into the gulf, and that there is a  
389 seasonal flow reversal, but with the transport flowing most of the year into the gulf, and only  
390 out of the gulf during fall (figures 9, and 12). The phase of the transport in the surface layer  
391 (the transport is essentially in phase all along the gulf) also agrees rather remarkably well with  
392 the phases of surface geostrophic velocities estimated by Ripa and Marinone (1989), Ripa  
393 (1990) and Navarro et al. (2016, see their fig. 6b) with maximum inflow and outflow in  
394 summer and fall, respectively. Ripa (1997) only considered the annual frequency, but the  
395 annual fit to the observations and the associated Kelvin wave model, also have a maximum  
396 inflow of the mean surface velocity in the summer. We have also found that this three-layer,  
397 near-surface, mean circulation extends most of the gulf's length starting at the mouth (figure  
398 5). The mean winds are towards the mouth (Bordoni et al., 2004), which is coincident with the  
399 mean winds used to force the HYCOM (not shown). However, the mean transport in the  
400 surface layer is towards the north, contrary to the mean winds. Furthermore, the seasonal  
401 cycle of the winds shows that they only flow towards the north in summer and towards the  
402 south the rest of the year (Bordoni et al., 2004; Collins and Castro, 2022). Therefore, the  
403 mean and seasonal transport of the surface layer does not appear to be directly forced by the  
404 local winds, highlighting the role of the eastern tropical Pacific Ocean in the circulation of the  
405 gulf, which also has been found to be important in the coastal circulation along the western  
406 Mexican coast (Gómez-Valdivia et al, 2015).

407 We have already mentioned the good agreement between figure 2 and the corresponding  
408 figure 3d in Collins and Castro (2022). These authors, also calculated the across-gulf  
409 integrated transport at the mouth of the gulf in the upper 400 m. They also have an inflowing  
410 surface layer down to about 150 m, and an outflowing layer from 150 m down to 400 m, but  
411 there is not an inflowing third layer, at least down to 400 m. We also found a general  
412 qualitative agreement between figure 2 and a corresponding seven-year mean, modeled  
413 velocity by Zamudio et al. (2008). There are, however, some important differences. Most  
414 notably, they do not obtain the small surface inflow on the western side, their western outflow  
415 core is not adjacent to the coast and it is surface intensified; and their subsurface, eastern  
416 outflow region is somewhat larger. Some of these differences may be due to the fact that they

417 computed a seven-year mean, as compared to just one year in here; but some differences  
418 may also stem from the smaller vertical resolution they used (20 layers).

419 The Mexican Coastal Current (MCC) is a subsurface poleward flow adjacent to the west coast  
420 of Mexico. At  $\sim 17^\circ\text{N}$  the current also flows at the surface and reaches the mouth of the gulf  
421 (Kessler, 2006; Lavín et al., 2006; Godínez et al., 2010; Gómez-Valdivia et al., 2015; Portela  
422 et al., 2016). Figure 2 is consistent with the poleward flow in the eastern part of the section.  
423 The poleward flow through the eastern side is present in the first three layers where the mean  
424 transport flows in alternating directions (figures 2 and 4), but the across-gulf integrated  
425 transport in the second layer is equatorward (figure 3 and table 1). Therefore, in the second  
426 layer, the transport coming out from the gulf is larger than the inflowing transport from the  
427 MCC. The outflow in the second layer is concentrated in a subsurface core centered at  $\sim 100$   
428 m which is stronger and more concentrated than the shallower poleward flow over the  
429 continental shelf on the eastern side (figure 2).

430 The seasonal variation of the MCC is poorly known. Kessler (2006) and Portela et al. (2016)  
431 identified the strongest poleward flow reaching the gulf in summer. Gómez-Valdivia et al.  
432 (2015), using a numerical model, found a semiannual variation of the current with maxima in  
433 spring and fall, associated to the arrival of coastally trapped waves from the equator. Figure 7  
434 shows that there is poleward flow through the eastern part of the gulf all year round, with  
435 largest velocities in summer and smallest in winter. Assuming that the MCC at the gulf's  
436 entrance covers layers one, two, and, possibly, part of the third (table 1), then figure 10 and  
437 figure 11a, and similar figures for layers 2 and 3 (not shown), show that there is, indeed, a  
438 strong semiannual signal, although concentrated more on the western side of the mouth of  
439 the gulf. On the eastern side, where the MCC flows into the gulf, there is a significant  
440 contribution from the semiannual harmonic with the greatest inflow in summer and the  
441 greatest outflow in spring. There are smaller maxima and minima in winter and fall,  
442 respectively, which are more evident in the combined seasonal cycle of layers 1 and 2 (not  
443 shown).

444 Figures 10 and 11b strongly suggest a westward propagation west of  $108^\circ\text{W}$  at the mouth of  
445 the GC, which is highlighted by the sloping black line in figure 10a. The slope of that line gives  
446 a very small propagation speed of 0.7 cm/s. To see if this could correspond to a Rossby wave

447 of semiannual frequency, we calculated the parameters of such a wave. The critical  
448 (minimum) period of a Rossby wave depends on latitude and coastal orientation (Clarke and  
449 Shi, 1991). Around the mouth of the gulf, Clarke and Shi (1991) calculated two very different  
450 critical periods of 172.4 and 260.3 days. To allow for the propagation of the semiannual  
451 frequency we will take the lower critical period which corresponds to an almost meridional  
452 coastline. For that period, the internal radius of deformation can be obtained from the  
453 expression of the maximum critical frequency of Rossby waves for a meridional coastline,  
454 namely  $a = 2\omega_c/\beta$ , where  $\omega_c$ , corresponds to the critical frequency (*i.e.*, the frequency  
455 corresponding to the critical period of 172.4 days), and  $\beta$  is the meridional gradient of the  
456 Coriolis parameter. Taking the value of  $\beta$  at the mouth of the gulf gives  $a = 40.2 \text{ km}$ , which  
457 corresponds to a first mode, internal gravity wave propagation speed of  $2.33 \text{ m/s}$ . With the  
458 value of  $a$  we can calculate the wavelengths and phase speeds of the corresponding long,  
459 and short, purely westward (phase propagation) Rossby waves at the semiannual frequency.  
460 The values are 355.5 km and phase speed of 2.3 cm/s for the long wave, and 179.2 km and  
461 phase speed of 1.1 cm/s, for the short wave. For the phase speed of 0.7 cm/s inferred from  
462 figure 10a, the corresponding wavelength for the semiannual frequency is 110.4 km.  
463 Therefore, the propagating pattern in figures 10 and 11, corresponds much more closely to  
464 the short Rossby wave, and given the uncertainties in the values of the Rossby radius of  
465 deformation, and in the empirical estimation of the phase speed from figure 10a, this seems  
466 like a reasonable approximation.

467 The calculation of the net outflowing, laterally integrated transport, enables us to estimate a  
468 lower bound for the turnover time of the gulf (Talley et al., 2011). The net outflowing transport  
469 is essentially the same as the inflowing transport, the small difference being the water  
470 evaporated in the gulf. From table 1, the sum of the outflowing transport is  $0.2972 Sv$ . The  
471 volume of the gulf delimited by the zonal mouth used in this work, is  $1.3119 \times 10^{14} \text{ m}^3$ .  
472 Dividing the volume by the outflowing transport gives a lower bound for the turnover time of  
473 approximately 14 years.

474 We have estimated the laterally integrated transport across the mouth of the gulf, and all the  
475 way to the bottom using a global, one-year simulation of the HYCOM. Using a global model  
476 ensures that the effects of the Pacific Ocean on the gulf are incorporated. The transport of the  
477 three upper layers compares qualitatively well with the limited available observations. The

478 same upper three layers found at the mouth, are present in almost all the length of the gulf,  
479 with approximately the same thickness. The transport in the surface layer inside the gulf is  
480 almost everywhere greater than the one at the mouth, producing mean upwelling into the  
481 surface layer. This upwelling may explain the biologically rich waters of the gulf. In the  
482 surface layers, there is a concentrated outflow on the western side of the mouth of the gulf,  
483 and a broader inflow on the eastern side. The greatest seasonal exchange of the gulf with the  
484 Pacific Ocean above 820 meters occurs in summer and fall, with outflow in summer and  
485 inflow in fall, except for the surface layer where inflow and outflow are reversed with respect  
486 to the layers below. We have found that there is a strong semiannual signal in the seasonal  
487 variation of the transport, with a stronger semiannual signal concentrated in the western  
488 outflow. In the deeper layers (below 380 m) the semiannual signal on the western side is  
489 consistent with the propagation of a short Rossby wave. From the results of this work, we  
490 have left some unanswered questions which lie outside the scope of this article. More  
491 significantly, we have not addressed the causes of the water exchange found in the model,  
492 and the origins of the possible Rossby wave, both of which probably involve dynamics of the  
493 equatorial and eastern Pacific Ocean, which are left for future research.

494

#### 495 **Acknowledgments**

496 This work was partially funded through a graduate scholarship granted to Gonzalo Acosta-  
497 Solís by CONAHCyT. The HYCOM simulation was performed at the Navy Department of  
498 Defense (DoD) Supercomputing Resources at Stennis Space Center, Mississippi, using  
499 grants of computer time from the DoD High Performance Computing Modernization Program.  
500 The comments by the two anonymous reviewers improved the manuscript.

501

#### 502 **References**

503

- 504 Acosta-Solís, G. (2023). El Golfo de California visto a través del modelo numérico Global  
505 HYCOM. M.S. Thesis. CICESE. 51 pp
- 506
- 507 Badan-Dangon, A., & C. J. Koblinsky, and T. Baumgartner (1985). Spring and summer in the  
508 Gulf of California: Observations of surface thermal patterns. *Oceanol. Acta*, 8, 1.
- 509

- 510 Baumgartner, T. R., & N. Christensen (1985). Coupling of the Gulf of California to large-scale  
511 interannual climatic variability. *J. Mar. Res.*, 43: 825-848.  
512
- 513 Beron-Vera, F. P., & Pedro Ripa (2000). Three-dimensional aspects of the seasonal heat  
514 balance in the Gulf of California. *J. Geophys. Res.*, 105, C5: 11,441-11,457.  
515
- 516 Bordoni, S., P. E. Ciesielski, R. H. Johnson, B. D. McNoldy, & B. Stevens (2004). The low-  
517 level circulation of the North American Monsoon as revealed by QuikSCAT. *Geophys. Res.*  
518 *Let.* 31, L10109. doi:10.1029/2004GL020009  
519
- 520 Bray, N. A. (1988). Thermohaline Circulation in the Gulf of California. *J. Geophys. Res.*, 93,  
521 C5: 4993-5020.  
522
- 523 Buijsman, M. C., B. K. Arbic, J. G. Richman, J. F. Shriver, A. J. Wallcraft, & L. Zamudio  
524 (2017). Semidiurnal internal tide incoherence in the equatorial Pacific, *J. Geophys. Res.*  
525 *Oceans*, 122, 5286–5305. doi:10.1002/2016JC012590.  
526
- 527 Castro, R., M. Lavín, & P. Ripa (1994). Seasonal heat balance in the Gulf of California. *J.*  
528 *Geophys. Res.*, 99, C2: 3249–3261.  
529
- 530 Castro, R., Reginaldo Durazo, Affonso Mascarenhas, Curtis A. Collins, & A. Trasviña (2006).  
531 Thermohaline variability and geostrophic circulation in the southern portion of the Gulf of  
532 California. *Deep Sea Res. I*, 53: 188-200.  
533
- 534 Castro, R., C. A. Collins, T. A. Rago, T. Margolina, & L. F. Navarro-Olache (2017). Currents,  
535 transport, and thermohaline variability at the entrance to the Gulf of California (19–21 April  
536 2013). *Cien. Mar.*, 43, 3. doi: <http://dx.doi.org/10.7773/cm.v43i3.2771>  
537
- 538 Clarke, A.J., & Shi, C (1991). Critical frequencies at ocean boundaries. *J. Geophys. Res.*, 96,  
539 C6.  
540
- 541 Collins, C.A., & R. Castro (2022). Observations of the exchange of ocean waters between  
542 the Pacific Ocean and the Gulf of California. *Ocean and Coastal Res.*, v70(suppl 1):e22040.  
543 doi: <http://doi.org/10.1590/2675-2824070.22036cac>  
544
- 545 Godínez, V. M., E. Beier, M. F. Lavín, and J. A. Kurczyn (2010), Circulation at the entrance of  
546 the Gulf of California from satellite altimeter and hydrographic observations, *J. Geophys.*  
547 *Res.*, 115, C04007, doi:10.1029/2009JC005705.  
548
- 549 Gómez-Valdivia, F., A. Parés-Sierra, & A.L. Flores-Morales (2015). The Mexican Coastal  
550 Current: A subsurface seasonal bridge that connects the tropical and subtropical Northeastern  
551 Pacific. *Cont. Shelf Res.*, 110: 100–107. doi: <http://dx.doi.org/10.1016/j.csr.2015.10.010>  
552
- 553 Kessler, W. S. (2006). The circulation of the eastern tropical Pacific: A review. *Prog.*  
554 *Oceanogr.* 69: 181–217. doi:10.1016/j.pocean.2006.03.009  
555
- 556 Lavín, M. F., R. Durazo., E. Palacios., M.L. Argote, & L. Carrillo (1997). Lagrangian

557 observations of the circulation in the northern Gulf of California. *J. Phys. Ocean.* 27, 239-246.  
558  
559 Lavín, M. F., & S. G. Marinone (2003). An Overview of the Physical Oceanography of the Gulf  
560 of California. In O.U. Velasco, J. Sheinbaum & J. Ochoa (Eds) *Nonlinear Processes in*  
561 *Geophysical Fluid Dynamics*. Chap. 11. Kluwer Academic Publishers.  
562  
563 Lavín, M. F., E. Beier, J. Gómez-Valdés, V. M. Godínez, and J. García  
564 (2006), On the summer poleward coastal current off SW México, *Geophys.*  
565 *Res. Lett.*, 33, L02601, doi:10.1029/2005GL024686.  
566  
567 Lavín, M. F., R. Castro, E. Beier, & V.M. Godínez (2013), Mesoscale eddies in the southern  
568 Gulf of California during summer: Characteristics and interaction with the wind stress, *J.*  
569 *Geophys. Res. Oceans*, 118, 1367–1381, doi:10.1002/jgrc.20132  
570  
571 López, M., L. Flores-Mateos, & J. Candela (2021). Tidal currents at the sills of the Northern  
572 Gulf of California. *Cont. Shelf Res.*, 227, doi: <https://doi.org/10.1016/j.csr.2021.104513>  
573  
574 López, M., J. Candela, & M. L. Argote (2006). Why does Ballenas Channel have the coldest  
575 SST in the Northern Gulf of California? *Geophys. Res. Lett.*, 33, L11603).  
576 doi:10.1029/2006GL025908  
577  
578 Marinone, S. G. (1997). Tidal residual currents in the Gulf of California: Is the M2 tidal  
579 constituent sufficient to induce them? *J. Geophys. Res.*, 102, C4: 8611-8623.  
580  
581 Martínez Alcalá, Jose Antonio (2002), Modeling studies of mesoscale circulation in the Gulf of  
582 California. PhD Thesis, Oregon State University, 173 pp.  
583 [https://ir.library.oregonstate.edu/concern/graduate\\_thesis\\_or\\_dissertations/n296x2688?locale](https://ir.library.oregonstate.edu/concern/graduate_thesis_or_dissertations/n296x2688?locale=en)  
584 [=en](https://ir.library.oregonstate.edu/concern/graduate_thesis_or_dissertations/n296x2688?locale=en)  
585  
586 Mascarenhas Jr., A. S., R. Castro, C. A. Collins, & R. Durazo (2004). Seasonal variation of  
587 geostrophic velocity and heat flux at the entrance to the Gulf of California, Mexico. *J.*  
588 *Geophys. Res.*, 109, C07008. doi:10.1029/2003JC002124  
589  
590 Navarro, R., M. López, and J. Candela (2016), Seasonal cycle of near-bottom transport and  
591 currents in the northern Gulf of California, *J. Geophys. Res. Oceans*, 121, 8621-8634,  
592 doi:10.1002/2016JC012063.  
593  
594 Pegau, W. S., E. Boss, & A. Martínez (2002). Ocean color observations of eddies during the  
595 summer in the Gulf of California. *Geophys. Res. Lett.*, 29(9).  
596  
597 Portela E. et al. (2016). Water Masses and Circulation in the Tropical Pacific off Central  
598 Mexico and Surrounding Areas. *J. Phys. Oceanogr.*, 46, 10. doi: 10.1175/JPO-D-16-0068.1  
599  
600 Ripa, P., and S. G. Marinone (1989), Seasonal variability of temperature, salinity, velocity,  
601 vorticity and sea level in the central Gulf of California, as inferred from historical data, *Q. J. R.*  
602 *Meteorol. Soc.*, 115, 887-913.

- 603 Ripa, P. (1990), Seasonal circulation in the Gulf of California, *Ann. Geophys.*, 8(7-8), 559-  
604 564.
- 605
- 606 Ripa, P. (1997). Towards a physical explanation of the seasonal dynamics and  
607 thermodynamics of the Gulf of California. . *J. Phys. Oceanogr.*, 27: 597–614.
- 608
- 609 Talley, L.D., G.L. Pickard, W.J. Emery, & J.H. Swift (2011). *Descriptive Physical*  
610 *Oceanography*, Sixth Ed. Academic Press. doi: <https://doi.org/10.1016/C2009-0-24322-4>
- 611
- 612 Zamudio, L., P. Hogan, & E. J/ Metzger (2008). Summer generation of the Southern Gulf of  
613 California eddy train. *Jour. Geophys. Res.*, 113, C06020. doi:10.1029/2007JC004467
- 614
- 615 Zamudio, L., E. J. Metzger, & P. J. Hogan (2010). Gulf of California response to Hurricane  
616 Juliette. *Ocean Modelling*, 33: 20-32.
- 617
- 618 Zamudio, L., E. J. Metzger, & P. Hogan (2011). Modeling the seasonal and interannual  
619 variability of the northern Gulf of California salinity, *J. Geophys. Res.*, 116, C02017,  
620 doi:10.1029/2010JC006631